Journal of Constructional Steel Research 194 (2022) 107334

Contents lists available at ScienceDirect

Journal of Constructional Steel Research

journal homepage: www.elsevier.com/locate/jcsr

# Improved design method for interaction buckling resistance of welded box-section columns

M. Radwan *, B. Kövesdi

*Budapest University of Technology and Economics, Department of Structural Engineering, Műegyetem rkp. 3., 1111 Budapest, Hungary.*

ARTICLE INFO

*Keywords:*
Interaction buckling
Improved resistance
Plate buckling
Flexural buckling
Welded box-section
Numerical simulation

ABSTRACT

The current paper studies the global and local interaction behaviour of box-section columns using numerical simulations by creating a numerical model and analysing their buckling resistances to pure compression. The developed numerical model uses a combination of global and local imperfections as well as residual stresses, which are the key parameters of the resistance calculation. The unique approach in the current paper is that all the previous studies applied safe sided imperfections, while this research applies improved imperfections for the local buckling behaviour provided by the authors in previous research work. This improved local geometric imperfection is applied in the verified numerical model to determine and analyse the interaction buckling resistance and develop an improved design resistance calculation method. Based on the accurate numerical simulation results, an analytical design approach following the buckling resistance calculation methodology of the Eurocode has been developed in the current paper and proposed for application. A comparison is made with the available design methods found in the international literature showing the achieved improvements.

## 1. Introduction

Welded box sections are widely used nowadays due to their manufacturing and fabrication advantages, making them a practical structural element in many constructions. This puts an extra demand on a more practical understanding of their structural behaviour in a wide range of geometrical configurations. The stability behaviour is one of the factors that need more attention as it affects the ability of sections to resist the load and causes ineffective utilisation of the section capacity. The stability issues for this section can be classified into three types, namely the global, local and interaction buckling behaviours. The global buckling is categorised by a large deformation near the weakest point along the length of the column, depending on its configuration. These deformations will hinder the ability of the column to sustain further loading. The local buckling is categorised by a group of half-sin waves that appears at the different plates of the section that has a very high width to thickness ratio, and this will cause a significant decrease in the resistance of the section to resist loads by not allowing the section to reach the plastic resistance and the full yielding of the section. The third type is interaction buckling which is a combination of the previously mentioned two types of buckling that will occur in the case of sections that are slender both globally and locally. While many researchers investigated the global and local buckling of the box sections, only limited efforts have been paid to study the interaction behaviour between these two types of buckling and provide a more advanced approach to estimate the interaction buckling resistance. The current research aims to investigate the behaviour of welded box-section columns under pure compression by applying GMNIA (geometrically and materially nonlinear analysis with imperfections) and propose a reliable design method to give a more accurate resistance.

The current Eurocode utilises a simplified approach to estimate the interaction buckling resistance. The global buckling reduction factor is based on the Ayrton-Perry-type formula that was developed and calibrated to estimate the global buckling resistance of columns based on a set of curves given in EN1993-1-1 [1]. The currently adopted buckling curve for the analysed welded slender box-section columns is the buckling curve “b”. This curve was calibrated to account for the geometrical imperfections and residual stresses that exist in columns, and the characteristic value of the buckling resistance fits well with the numerical calculations using L/1000 geometric imperfections and additional residual stresses. The second reduction factor accounts for local buckling, which is based on the Winter-type buckling curve available in EN1993-1-5 [2]. The local buckling reduction factor can be used in the effective width method to reduce the cross-sectional area of

* Corresponding author.
*E-mail address:* mohammad.radwan@emk.bme.hu (M. Radwan).

https://doi.org/10.1016/j.jcsr.2022.107334
Received 22 January 2022; Received in revised form 11 May 2022; Accepted 11 May 2022
Available online 20 May 2022

the Class 4 sections (i.e., where the width-to-thickness ratio exceeds the given value) under compression. By multiplying these two factors, the cross-sectional area and the yield strength of the column, the characteristic interaction resistance of the section can be determined.

A limited number of researchers studied this interaction behaviour combining the global and local buckling behaviour of welded box-section columns. There is quite a large number of investigations in this topic studying the interaction behaviour of I-section columns. The most significant and recent results are given in [3, 4]. However, these results are not directly applicable to welded box-section columns. One of the most recent research on box-section columns was done by Schillo et al. [5], studying the interaction buckling of high strength steel columns. They proposed a new design formula based on numerical and experimental results. The proposed method utilised an equivalent geometrical imperfection that accounts for the effect of local buckling instead of the effective width method. The method utilises a similar approach as currently given in the Eurocode EN1993-1-1 [1] for global buckling, but with the addition of the equivalent imperfection to account for the loss of stiffness due to local buckling. The authors have mentioned that the Eurocode results are highly scattered compared to their numerical results. Another research on this topic was done by Degée et al. [6]. A numerical parametric study was carried out as well as an experimental test program to study the effect of interaction buckling. The authors suggested a modification factor of the global slenderness to include the ratio of the gross cross-sectional moment of inertia ($I$) and the effective moment of inertia ($I_{eff}$) to account for the loss of flexural stiffness when interaction buckling occurs and included the local plate reduction factor in the $\beta$ factor modifying the global slenderness $\bar{\lambda}_g$. Additionally, an upgrade from Eurocode curve "b" to curve "a" was also suggested as they have found that the buckling resistance of the class 4 welded box-section column is higher than what is currently adopted by the Eurocode. Both researchers criticised the currently adopted design formula of the Eurocode and suggested further investigation to be done over a larger global and local slenderness range. Both are investigated in the current paper and the improved design procedures will be validated against the current numerical results in a wide slenderness range.

The presented research program starts by creating a numerical model that utilises the GMNIA (Geometrically and Materially Nonlinear analysis) technique to estimate the interaction buckling resistance of the box-section columns. The model uses a certain combination of local and global imperfections and residual stress to give an accurate estimation of the buckling resistance. This is the first point where the current research delivers a significant new contribution because the applicable imperfections for the global and for the local buckling behaviour have been separately investigated and improved by the authors [7]. The current paper takes advantage of these previous investigations, making it possible to determine the interaction buckling resistance more accurately. The applied imperfection combinations include always L/1000 as global imperfection and local imperfections specified based on the local slenderness of the cross-section calibrated for the plate buckling curve of the second-generation Eurocodes (prEN 1993-1-5:2024 [8]). As previously validated by the authors, this buckling curve provides a more reliable and accurate estimation of the local buckling resistance of box-section columns compared to the Winter-type curve that is available in the ancient EN1993-1-5, which was criticised by different researchers to provide overestimated results. It also means that if the buckling curve related to local buckling is changed, the applied imperfections in the numerical model should also be changed following the buckling curve change and accounting for accurate results. The applied geometric imperfections are combined with residual stresses according to the ECCS residual stress patterns representing light welding [9]. The same residual stresses are recommended in the second-generation Eurocodes prEN 1993-1-14 [10] as well. The developed numerical model is also validated against tests available in the literature and utilised to perform a parametric study on a wide range of global and local slenderness for different steel grades between S235 and S960. Based on the numerical parametric study, the interaction buckling resistance of the analysed columns are determined for a wide parameter range of local and global slenderness, which forms a database that is the source for a detailed investigation of the structural behaviour of the interaction buckling resistance and improved design method development, which is the second main new contribution of the current paper. The reason why previous design methods show larger scatter are highlighted, and a reduction factor for the interaction buckling has been developed considering the local and global slenderness ratio of the analysed columns, taking the nonlinear interaction behaviour into account.

## 2. Literature review

### 2.1. Eurocode-based design approach

#### 2.1.1. Global buckling resistance

Verification against buckling according to EN 1993-1-1 [1] is executed by Eq. (1):

$$\frac{N_{Ed}}{N_{b,Rd}} \leq 1 \tag{1}$$

where: $N_{Ed}$is the design value of the compression force, $N_{b,Rd}$is the design buckling resistance of the compression member. For class 4 cross-sections in which the local buckling occurs before the attainment of yield stress in one or different parts of the cross-section, the design buckling resistance of compression elements can be determined as follows according to Eq. (2):

$$N_{b,Rd} = \frac{\chi A f_y}{\gamma_{M1}} \tag{2}$$

where: $\chi$ is the reduction factor for the relevant buckling mode determined according to Eqs. (3)–(4).

$$\chi = \frac{1}{\phi + \sqrt{\left(\phi^2 - \bar{\lambda}_g{}^2\right)}} \leq 1.0 \tag{3}$$

$$\phi = 0.5\left[1 + \alpha\left(\bar{\lambda}_g - 0.2\right) + \bar{\lambda}_g{}^2\right] \tag{4}$$

where:

$\alpha$ is the imperfection factor; in this study, equal to 0.34, corresponding to the buckling curve b according to EN1993–1- [1].

The non-dimensional slenderness $\bar{\lambda}_g$ can be determined according to Eq. (5), where $N_{cr}$is the elastic critical force for the relevant buckling mode based on the properties of the cross-section.

$$\bar{\lambda}_g = \sqrt{\frac{A f_y}{N_{cr}}} \tag{5}$$

#### 2.1.2. Local buckling resistance

According to EN1993-1-5 [2], class 4 sections are those plates and structures which are susceptible to local buckling. They cannot attain their elastic resistance and are characterised by local buckling failure. The various method can be used to design these types of cross-sections, such as the reduced stress method or the effective width method. The latter is investigated in the current paper. The effective width method works by reducing the effective area of the compression zone of the plate, according to Eq. (6), as the applied stresses on the non-effective regions are carried out by the adjacent effective areas.

$$A_{c,eff} = \rho A_c \tag{6}$$

Where: ρ is the reduction factor for plate buckling.

For the case of square box-section columns with all elements considered as internal compression elements, the reduction factor ρ may

be taken by Eqs. (7)–(8):

$$\rho = \begin{cases} 1, \ \lambda_\rho < 0.673 \\ \dfrac{\bar{\lambda}_p - 0.005(3+\psi)}{\bar{\lambda}_p^2} \le 1, \quad \lambda_\rho \ge 0.673 \end{cases} \tag{7}$$

$$\bar{\lambda}_p = \sqrt{\frac{f_y}{\sigma_{Cr}}} = \frac{\bar{b}/t}{28.4\varepsilon\sqrt{k_\sigma}} \tag{8}$$

where:

Ψ is the stress ratio.

$\bar{b}$ is the appropriate width to be taken according to Table 5.2 of EN 1993-1-1 [1],

$k_\sigma$ is the buckling factor corresponding to the stress ratio Ψ and boundary conditions for long plates $k_\sigma$ is given in Table 4.1 or Table 4.2 of Eurocode3 [1],

t is the thickness,

$\sigma_{Cr}$ it is the elastic critical plate buckling stress,

ε calculated according to Eq.(9)

$$\varepsilon = \sqrt{\frac{235}{f_y\left[\frac{N}{mm^2}\right]}} \tag{9}$$

### 2.1.3. Interaction buckling resistance

In EN1993-1-1 [1], the interaction buckling is accounted for by taking both the effect of the global and local buckling. The effect of global buckling is taken by calculating the global reduction factor $\chi$ according to Eq.(3). Also, the effect of local buckling by calculating the effective area by the effective width method according to Eq. (6). Both effects will be combined by multiplication according to Eq. (2) without taking into account the interaction that can happen between the two buckling modes. The final equation will be as follows:

$$N_{b,Rd} = \frac{\chi A_{eff} f_y}{\gamma_{M1}} = \frac{\chi \rho A f_y}{\gamma_{M1}} \tag{10}$$

A certain interaction is, however, considered within the calculation of the global slenderness ratio according to Eq. (10), where the effective cross-sectional area is used instead of the gross cross-sectional area for class 4 cross-sections. It leads to the fact that if the considered cross-sectional area reduces, the slenderness of the column will be smaller, leading to a larger global reduction factor and buckling resistance. This interaction consideration method has been criticised by researchers in the past, and several modifications have been already proposed, as summarized in the following section.

## 2.2. Previous research results

Degée et al. [6] studied the interaction buckling behaviour of S355 welded rectangular section columns (RHS). A total number of six samples were tested in this investigation with global slenderness of 0.35, 0.55, and 0.75 for the same local slenderness of 0.9. A numerical parametric study was also carried out for the global slenderness of 0.8 to 1.4 and local slenderness of 0.7 to 1.1 to study the interaction buckling resistance of welded rectangular sections columns. The authors suggested the application of *L/1000* as global imperfection and *b/1000* as a local imperfection if the residual stresses are also applied. Otherwise, *L/750* as a global imperfection and *b/250* as local imperfection can be used. The authors suggested an upgrade of the buckling curve from Eurocode buckling curve "b" to curve "a" as the buckling curve "b" was found too conservative. The authors suggested a new definition of global slenderness to account for the loss of stiffness due to the local slenderness and called it interaction slenderness $\bar{\lambda}_{int}$, and a new method was proposed for both normal and high strength steel structures, namely for S355, S460 and S690 steel grades. It is based on the Eurocode $\beta$ factor with the additional modification on the global slenderness to include the ratio of the gross moment of inertia to the effective moment of inertia ($\frac{I}{I_{eff}}$) The original $\beta$ factor contained only the ratio of effective area to the gross cross-sectional area ($\frac{A_{eff}}{A}$). Moreover, the effect of the local slenderness was adopted in the modification of the global slenderness, this will lead to decreasing the value of the global slenderness, and a larger resistance will be obtained due to the smaller slenderness as the reduction factor is increased.

This evaluation method includes the following steps: (i) calculation of the global slenderness according to Eq. (11), then by using the Eurocode EN1993-1-1 [1] the global reduction factor $\chi_a$can be determined by using $\bar{\lambda}_{GL}$and buckling curve "a", (ii) calculation of the local reduction factor $\rho_p$ using the plate buckling curve of EN1993-1-5 [2], (iii) modification of the global slenderness using the parameter $\beta$ given by Eq.(12) to obtain the $\bar{\lambda}_{int}$ as depicted in Eq. (13), (iv) then, using the interaction slenderness $\bar{\lambda}_{int}$ the overall reduction factor $\chi_a$ can be calculated using buckling curve "a" of EN1993-1-1 [1]. Finally, the design resistance can be obtained using Eq. (14).

$$\bar{\lambda}_{GL} = \sqrt{\frac{N_{Rk}}{N_{cr}}} = \sqrt{\frac{A f_y}{\pi^2 \frac{EI}{L_{cr}^2}}} \tag{11}$$

$$\beta = \frac{i}{i_{eff}} . \left[1 - 0.5\,\chi_a \left(1 - 0.6.\sqrt{\rho_p}\right)\right] \tag{12}$$

$$\bar{\lambda}_{int} = \beta . \bar{\lambda}_{GL} \tag{13}$$

$$N_{Rd} = \frac{\chi A_{eff} f_y}{\gamma_1} \tag{14}$$

Where $N_{cr}$ is the elastic critical force for the relevant buckling mode based on the gross cross-sectional properties, $i$ is the gross radius of gyration, and $i_{eff}$ is the effective radius of gyration, which is calculated as $\sqrt{\frac{I_{eff}}{A_{eff}}}$, where $I_{eff}$ is the effective moment of inertia in pure bending and $A_{eff}$ is the effective area in pure compression calculated according to EN1993-1-5 [2].

Khan et al. [11] investigated the structural behaviour and buckling resistance of slender box-section columns manufactured from HSS (690 MPa). Fifteen test specimens are examined, and buckling resistances are compared to various international standards, including the Eurocode, AISC, and Australian Standard. In this experimental program, only three tests failed in pure local buckling, while other tests failed in global or interaction buckling modes. The authors investigate the effects of residual stresses on the member capacity using heavy and light welds. A numerical model was also developed to carry out a numerical parametric study. In the study, L/1000 was used as global imperfection and b/1000 as local imperfection with residual stress. The numerical model was validated against experimental tests showing reliable results. Based on the experimental and numerical results, it was found that specimens with large global slenderness failed in global buckling, specimens with small global slenderness failed due to local buckling. Intermediate specimens failed due to a combination of both the global and local buckling. Accordingly, the authors suggested utilising a reduction factor that accounts for the combined buckling effect. It was stated that all normalized values of the experimental and numerical tests were lying above the buckling curve "b" of the Eurocode and suggested utilising this curve as a suitable curve for determining the interaction buckling. It was also noticed there was no significant difference between specimens with heavily and lightly welded sections.

Yang et al. [12] investigated numerically and experimentally the interaction buckling behaviour of welded box-section columns. Twelve steel columns with medium lengths were tested. Two specimens were welded square hollow section (SHS) and ten with welded rectangular hollow sections (RHS). Tests specimens were made of S235 and S355. All

specimens under this experimental program failed due to the interaction buckling between the local and the global buckling modes. Local buckling occurred first and became more obvious before reaching the ultimate load. The authors found that the high slenderness ratio of the plate led to an early local buckling that resulted in a lower ultimate bearing capacity. It was found that the current specifications are not taking into account the post-buckling capacity of the plates and, therefore, estimate a lower interaction buckling resistance. The post-buckling behaviour should be taken more accurately into account to achieve an economical design. A numerical parametric study was performed on normal and high strength steel columns. Based on the numerical study, the authors suggested using the buckling curve "a" of Eurocode instead of the buckling curve "b" for S960 steel grades. The Eurocode overestimates the buckling resistance of the welded box-section columns, indicating that the effective width method overestimates the local buckling resistance. It was also noticed that there is a significant influence of residual stresses on the ultimate capacity that can reach up to 20% in the case of medium length columns. Also, the initial imperfections mainly affect plates with a high slenderness ratio with an influence that can reach 10%.

Two experiments on S460 and S690 box-section steel columns were conducted by Usami and Fukumoto [13] to investigate the interactive buckling behaviour of high strength steel columns. An experimental study is carried out on the local and overall interaction buckling behaviour of welded built-up box columns made of high strength steel. Twenty-seven box-section columns with large slenderness were tested, twenty-four were loaded concentrically, and the rest were loaded eccentrically. Using the test results, an empirical design formula was presented to estimate the interaction buckling strength. Another experimental program [14]was executed by the same authors on a total of twenty-five columns with different lengths and width-to-thickness ratios. Both square and rectangular box sections were tested. A computer program was developed that uses the effective width method to investigate the collapse and characteristics of beam-columns that are suspectable to local buckling. The authors found that there is a good agreement between the results of the theoretical based computer program and the experimental test results for columns with large width-to-thickness ratio.

Chiew et al. [15] performed 17 tests on welded thin-walled box section steel columns made of S235 steel grade. The experimental programs included different sample configurations, including eccentric and concentric compressive loadings. This led to various failure modes, including local, overall and interaction buckling. The authors found that the effect of the plate width-to-thickness ratio and the column slenderness have a significant effect on the ultimate load-carrying capacity. The behaviour of long columns with a low width-to-thickness ratio was mainly dominated by overall buckling, while for sections with high width to thickness ratio failed due to the combined effect of local and overall buckling, i.e., interaction buckling. The authors suggested an iterative theoretical method to obtain the load and global slenderness curves for different columns under different load conditions utilising an elastic-perfectly plastic stress-strain diagram to calculate the stresses and the iterative load based on the curvature, neutral axis and the total strain of each element. Based on this method, a set of curves can be developed for moment-slenderness ($M$-$\lambda$) and load-slenderness ($P$- $\lambda$) and moment-load ($M$-$P$) interaction curves.

Kwon et al. [16] performed a series of compression tests on welded rectangular hollow section (RHS) columns fabricated from 6.0 mm thick steel plates using a steel material with a nominal yield strength of 315 MPa. The ultimate strength of the compression members undergoing a nonlinear interaction between local and overall buckling was investigated experimentally and theoretically. The width-to-thickness ratio for the web and flange of test specimens was selected that the elastic local buckling stress of the section was low, and a significant post-buckling strength reserve was displayed before reaching the ultimate load. Strength formulas using the DSM method and accounting for local buckling are proposed for the design of welded section columns and beams based on test results for H-section, C-section, RHS and CHS columns, and H-section beams. A provision for the width-to-thickness ratio limit of welded RHS columns should be prepared, and the proposed strength formulas for DSM should be further calibrated against more test results of various grade steel sections before they are applied for practical use. In this method, the authors tried to extend the applicability of the direct strength method (DSM) to welded box-section columns. The DSM method incorporates empirical formulas and elastic buckling stress obtained by buckling analysis and utilises a non-reduced cross-section area instead of using effective areas. This formula considers the interaction between the global and local buckling modes as the authors have already investigated the interaction buckling of H-sections. A similar formula was adopted for box-sections with a small reduction due to the reason that plates of H-sections have a higher post-buckling reserve. *Eq. (*15*)* shows the utilised formula where $P_{nl}$ is the nominal load accounting for the interaction buckling. $P_{crl}$ is the elastic local buckling load calculated by the finite element method or finite strip method. $P_{ne}$ is the nominal column design load calculated according to Eurocode using the appropriate buckling curve. Eq.(16) shows the slenderness based on the nominal column design load and the elastic critical buckling load.

$$P_{nl} = \begin{cases} P_{ne}, \ \lambda \le 0.745 \\ \left(1 - 0.2\left(\frac{P_{crl}}{P_{ne}}\right)^{0.55}\right)\left(\frac{P_{crl}}{P_{ne}}\right)^{0.55} P_{ne}, \quad \lambda > 0.745 \end{cases} \tag{15}$$

$$\lambda = \sqrt{\frac{P_{ne}}{P_{crl}}} \tag{16}$$

Schillo et al. [5] performed thirteen tests on a square welded box-section columns with a high $b/t$ ratio made of S500 and S960 steel grades having various global slenderness. Numerical modelling of the tests was also done by Ansys finite element program, and the numerical model was validated against the test results. The validated numerical model was used to perform a parametric study, which was used to determine the reduction factors to design box-section columns under the interaction of both global and local buckling. A different approach was used to implement the local buckling behaviour by adding additional geometric equivalent imperfection depending on the effective width method. According to the authors, the proposed approach seems to be more conservative across the analysed slenderness range, and it is more distinct for eccentrically loaded columns, where the bending is more important. Although this method is developed for high strength steel structures, it is still a good alternative to compare with, as it utilises the currently adopted Eurocode formula based on the Ayrton-Perry-type formulation of the global buckling resistance. Additionally, the proposed formula was validated against test results. In this approach, the authors utilised an additional equivalent local imperfection ($e_p$) to be implemented in the global buckling formula to account for the loss of stiffness due to local buckling, instead of using the Eurocode approach, which is the effective cross-sectional method. The proposed value for the equivalent local imperfection is calculated according to Eq. (17).

$$ep = s\left[\left(\frac{1}{\chi_A} - 1\right) + \frac{1-\psi}{1+\psi}\left(\frac{1}{\chi_W} - 1\right)\right] \tag{17}$$

Where, ($s$) is equal to the moment of inertia ($I$) over the area of the section ($A$) multiplied by the distance from the neutral axis to the maximum fibre ($z$) $s = \frac{I}{A.z}$. The parameters $\chi_A$ and $\chi_W$ are factors derived using the effective width method $\chi_A = \frac{Aeff}{A}, \chi_W = \frac{W_{eff}}{W}$, $\psi$ is a factor that depends on the eccentricity of the load. In this current research program, only pure compression is studied; therefore, $\psi = 1$ is assigned. Eqs. (18)–(22) are given to calculate the interaction resistance of the box-section columns.

$$\lambda_{gs} = \sqrt{\frac{N_{ult}}{N_{crit}}} \tag{18}$$

$$N_{ult} = \frac{N_{pl}}{1 + \frac{1-\psi}{1+\psi}} \tag{19}$$

where, $N_{pl}$ is the plastic resistance.

$$\eta = \alpha\left(\bar{\lambda}_{gs} - 0.2\right) + \left(e_L + e_p\right).\frac{A}{W} \tag{20}$$

$W$ is the cross-sectional modulus, $\alpha$ is the imperfection factor depending on the buckling curve; in this case, it is equal to 0.34 (corresponding to buckling curve b).

$$\phi = \sqrt{\frac{1}{k_e}}.0.5\left[k_e + \eta.k_e + \bar{\lambda}_{gs}^2\right] \tag{21}$$

$k_e$ is the ratio between $N_{ult}$ to $N_{pl,}$ and for this research, it is always equals to 1 as all sections are subjected to pure compression.

$$\chi_{gs} = \sqrt{\frac{1}{k_e}}\left[\frac{1}{\phi + \sqrt{\phi^2 - \bar{\lambda}_{gs}^2}}\right] \tag{22}$$

The value of $\chi_{gs}$ is multiplied by the plastic resistance to obtain the interaction buckling resistance of the box-section columns.

### 2.3. Executed research strategy

The literature review shows that the interaction behaviour between global and local buckling needs further investigation as the current design procedures are usually underestimating the capacity of steel box-section columns under pure compression [5,6,16]. The weakness of all the previous numerical investigations is in consideration of the local imperfections because there are no reliable results regarding the applicable imperfection magnitude. The applicable global imperfections and residual stresses for box-section columns are mainly agreed upon and accepted by researchers in the past. However, for the local imperfections, reliable values fitting to the buckling curves are just currently developed by the authors [7], which results are applied here for the interaction buckling resistance calculation. A further weakness of the previous analytical investigations is using the Winter-type buckling curve of the EN 1993-1-5 for the local buckling resistance calculation, which is proved to be too optimistic for square box-sections. Therefore, in the second-generation Eurocodes, a new buckling curve is proposed [10] for this specific case. However, the influence of changing the buckling curve on the interaction resistance has not been studied before. Therefore, in the current research program, a detailed numerical parametric study is executed using a validated numerical model to investigate the interaction buckling behaviour and to determine the accurate buckling resistance. Based on the numerical study, an improved resistance calculation method is proposed. The following research program is executed and presented in the current paper:

1- A numerical model is developed and validated against laboratory test results to determine the buckling behaviour of box-sections columns.
2- The local buckling capacity of the box-sections is controlled according to the Annex B curve of the EN 1993-1-5 by imposing the actual imperfection back calculated according to the Annex B curve, developed by the authors in previous research [7]. It was shown that the Annex B curve is giving conservative results for very slender sections, therefore, a maximum allowable imperfection of ±b/125 is applied, according to European manufacturing tolerance, to achieve a more reliable local buckling capacity for welded square box-sections. Therefore, as a first step, the local buckling resistance of the analysed sections is determined for class 4 sections, and the necessary imperfection magnitudes are determined to achieve the most accurate buckling resistances.
3- The global buckling capacity is controlled by imposing a suitable global imperfection of L/1000 in case the residual stresses are applied, as was shown by different studies to show a reliable solution [6]. Therefore, as a second step, a global buckling resistance of non-slender cross-sections is determined by investigating the boundaries of the interaction buckling behaviour.
4- An extended numerical parametric study is performed on a wide range of global and local slenderness, analysing slender columns with slender cross-sections, determining the interaction of global and local buckling resistance. Within the numerical model, well-established global and local geometric imperfections and residual stresses according to ECCS recommendations are applied.
5- The structural behaviour is analysed, and the differences between the current design methods and the obtained results are evaluated and discussed.
6- A fitting technique is used to propose a new formula to estimate the interaction buckling resistance of box-sections with high accuracy.
7- The numerical results are also compared to the previous design proposals, and the accuracy of the improved design approach is demonstrated.

## 3. Numerical model development and verification

### 3.1. Numerical model development

A numerical model is developed using Ansys finite element software [17]. Four node thin shell elements are used in the numerical model, which is a full shell model, as shown in Fig. 1. Geometrical and material nonlinear analyses using imperfections (GMNIA) are used to determine the ultimate load of the columns under study. Two master nodes are defined and placed in the centre of gravity of the end cross-sections. Rigid diaphragms were used to link all the 6 DOFs between the master nodes and the nodes at the end cross-sections using rigid member links. The movement of one of the master nodes is restricted against translation in (UX, UY, UZ) global directions and restrained against rotation along the longitudinal axis (RZ), while the other master node is allowed to move in the UZ direction, allowing to apply the compression force on the column.

At first, mesh sensitivity analysis is performed to obtain an appropriate mesh size yielding accurate results in a reasonable time without being numerically expensive, as shown in Fig. 2. A suitable number of elements is adopted to ensure an appropriate application of residual stress patterns. A mesh sensitivity study is performed for the smallest and the largest plate width that will be used in the current study, and one example is presented in Fig. 2. The width of the plate of the cross-section governs the applied mesh size. Results of the mesh sensitivity analysis show that decreasing the mesh size leads to a decrease in the ultimate load of the column. This shows the significance of the discretisation error check that can be controlled by applying a suitable mesh size to yield the accurate ultimate load. For the presented example, 10 mm FE size was sufficient. In this case, the error is equal to 0.1% from the smallest possible analysed mesh size. For all other cases, the applied element number has been regulated to keep the same width-to-element number ratio.

Imperfections exist naturally in plates due to the fabrication and manufacturing processes. In the current study, local imperfection is modelled manually through modification of the perfect shape of the specimens. As the authors have found in previous research [7] based on a numerical parametric study, the first buckling mode leads to the lowest resistance. Therefore, the first buckling mode is modelled and considered as the dominant failure mode for local buckling. The modelling of the first buckling mode is done by defining the shape of the local imperfection as a continuous half sin-waves equals to the integer number that is found by dividing the length ($L$) of the plate by its width ($b$).

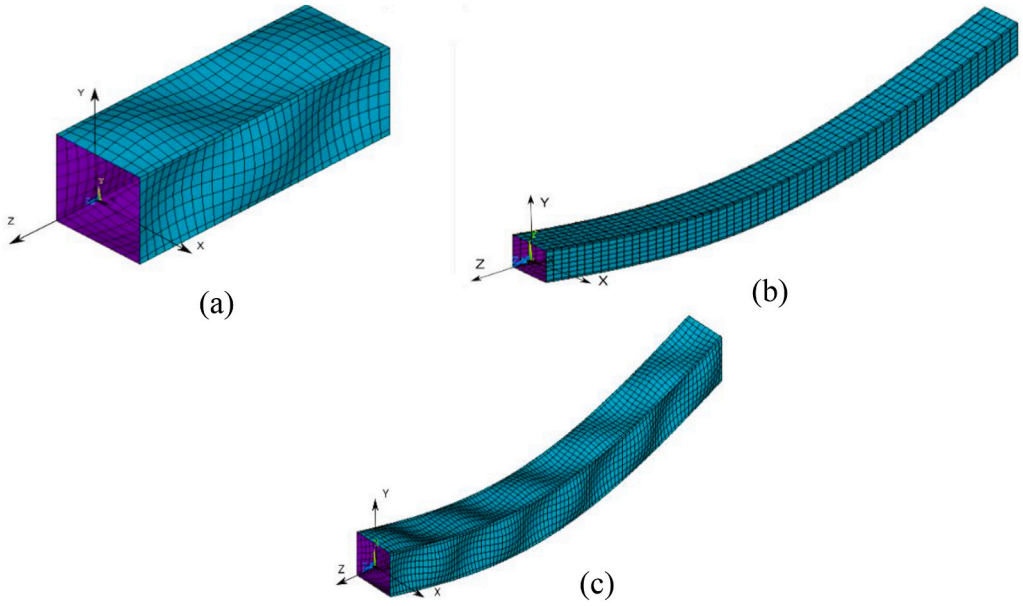


**Fig. 1.** a) Local, b) global, and c) interaction definitions of imperfections.

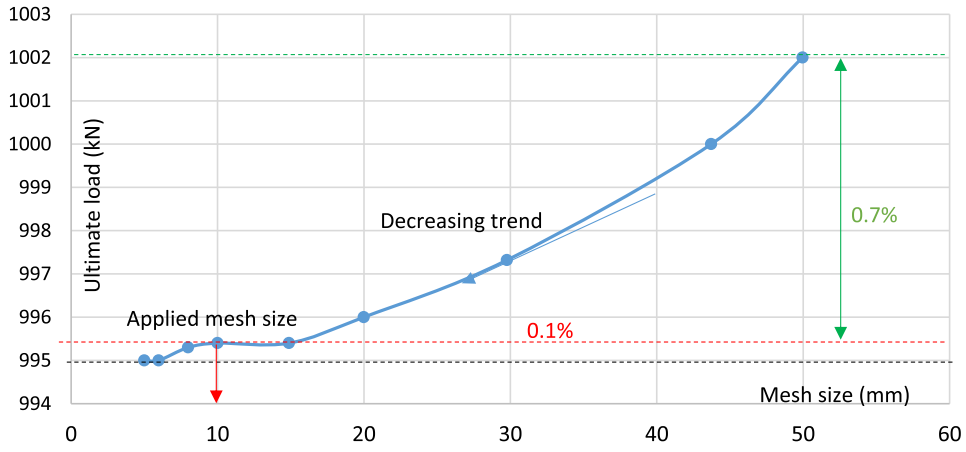


**Fig. 2.** The result of a mesh sensitivity analysis.

These half sin-waves are applied on each one of the columns along the longitudinal axis of each plate, with amplitudes having opposite signs on the adjacent sides. The shape of the local imperfection is defined in both directions (longitudinal and transversal) according to Eq. (23), and the shape of the global imperfection is defined according to Eq. (24), as shown in Fig. 3.

$$U_{L,Y}^{F} = U_{amp,loc}.sin\left(\frac{\pi.N_w.(i-1)}{N_c}\right) \tag{23}$$

$$U_{G,Y} = U_{amp,glob}.sin\left(\frac{\pi.(i-1)}{N_c}\right) \tag{24}$$

Where $U_{amp,loc}$ is the amplitude of the local imperfection (changed

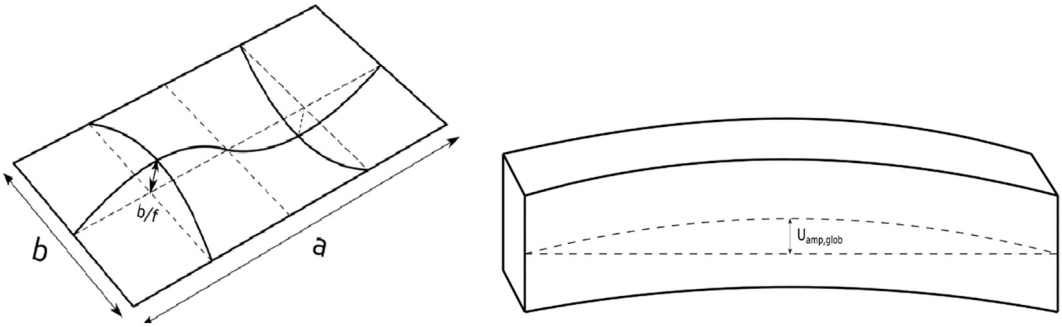


**Fig. 3.** Shape of local [7] and global imperfections.

during the numerical parametric study), while $U_{amp,glob}$ is the amplitude of the global imperfection (L/1000). *Nc* is the number of cross-sections defined along the length to model the different half sin-waves, $N_w$ is the number of half-sin waves along the length of the column (which is equal to the length $L$ over the width $b$), $i$ is the integer of the loop that goes from *1* to $N_c + 1$. The imperfections from Eq. (23–24) were added or subtracted to/from the proper coordinate of the defined nodes to model the imperfections at each node for each side of the column, depending on the sign of the imperfection and the location of the node. The full model for the three types of buckling is shown in Fig. 1, showing the different applied imperfections for global and local and their combination.

### 3.2. Applied material model

Two different material models are used for NSS and HSS materials, as they have different properties and behaviours. A quad-linear material model is used for NSS, as given by *Eqs.* (25)-*(30)* according to prEN 1993-1-14 [10] and presented in Fig. 4, is applied. This material model is accurately able to capture the yield plateau and the strain hardening behaviour of normal strength steel as proposed by Gardner et al. using a large database of coupon tests [18].

$$\sigma(\varepsilon) = \begin{cases} E\varepsilon, \ \varepsilon \le \varepsilon_y \\ f_y, \ \varepsilon_y < \varepsilon \le \varepsilon_{sh} \\ f_y + E_{sh}(\varepsilon - \varepsilon_{sh}), \ \varepsilon_{sh} < \varepsilon \le C_1\,\varepsilon_u \\ f_y C_1\varepsilon_u + \dfrac{f_u - f_y C_1\varepsilon_u}{(\varepsilon_u - C_1\varepsilon_u)}(\varepsilon - C_1\varepsilon_u), \quad C_1\,\varepsilon_u < \varepsilon \le \varepsilon_u \end{cases} \tag{25}$$

$$E_{sh} = \frac{f_u - f_y}{C_2\varepsilon_u - \varepsilon_{sh}} \tag{26}$$

$$\varepsilon_{sh} = 0.1\frac{f_y}{f_u} - 0.055 \; but \; 0.01 \le \varepsilon_{sh} \le 0.03 \tag{27}$$

$$\varepsilon_u = 0.6\left(1 - \frac{f_y}{f_u}\right), but \; 0.06 \le \varepsilon_u < A \tag{28}$$

$$C_1 = \frac{\varepsilon_{sh} + 0.25(\varepsilon_u - \varepsilon_{sh})}{\varepsilon_u} \tag{29}$$

$$C_2 = \frac{\varepsilon_{sh} + 0.4(\varepsilon_u - \varepsilon_{sh})}{\varepsilon_u} \tag{30}$$

To be able to use this model in Ansys APDL, different coefficients are needed, including the yield strain $\varepsilon_y = f_y/E$, strain hardening strain $\varepsilon_{sh}$, the strain hardening modulus $E_{sh}$, $A = 0.2$ which is the elongation after fracture defined according to material specification, $C_1$ "cut-off" strain coefficient defined to prevent over-predictions strength, and $C_2$ is defined in Eq. (26) to determine the slope of strain hardening $E_{sh}$. The calculated parameters for the steel grades under study are summarized in Table 1.

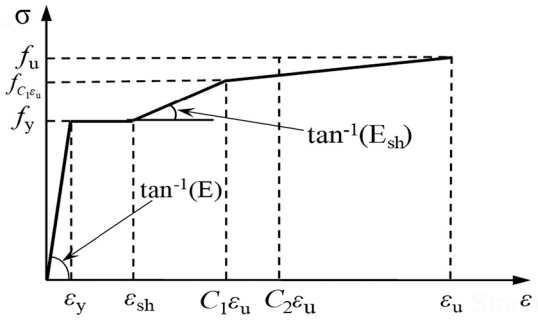


**Fig. 4.** NSS applied material model according to prEN 1993-1-14 [10].

**Table 1**
The applied material model parameters.

| | S235 | S355 | S460 |
|---|---|---|---|
| $f_y$ | 235 | 355 | 460 |
| $f_u$ | 360 | 510 | 540 |
| $\varepsilon_{sh}$ | 0.010 | 0.015 | 0.030 |
| $\varepsilon_u$ | 0.208 | 0.182 | 0.089 |
| $C_1$ | 0.287 | 0.310 | 0.505 |
| $C_2$ | 0.430 | 0.448 | 0.604 |
| $E_{sh}$ | 1578 | 2310 | 3407 |
| $C_1 \cdot \varepsilon_u$ | 0.060 | 0.057 | 0.045 |
| $f_{C1\varepsilon u}$ | 313 | 451 | 510 |

The Ramberg-Osgood-type material model, which is a nonlinear elastic-plastic material model using strain hardening, is applied in the numerical model to simulate the behaviour of HSS material according to Eq. *(31)*. Throughout this study, the factor $n = 14$ is used, which was determined by different coupon tests available in the international literature [19]. A modulus of elasticity of E = 210,000 and a Poisson's ratio $v$= 0.3 are used for all tests in this study. The yield and the ultimate strengths of the HSS material are summarized in Table 2. The characteristic behaviour of the three steel grades is shown in Fig. 5.

$$\varepsilon = \frac{\sigma}{E} + 0.002\left(\frac{\sigma}{fy}\right)^n \tag{31}$$

### 3.3. The applied residual stress model

Different studies have shown the correlation between the buckling capacity and the effect of both the residual stresses and imperfections. As for the slender plates, the effect of geometrical imperfections surpasses the influence of residual stress. The effect of residual stress still has a significant influence on the buckling capacity of columns under compression as it can cause loss of stiffness and premature yielding. Therefore, an accurate residual stress model must be carefully chosen to give an accurate estimation of the buckling capacity of the columns. Different research programs proposed different residual stress models [20,21]. A typical distribution of residual stress for welded box-sections that is reliable and leads to a good estimation of buckling resistance is shown in Fig. 5, ($\sigma_t$) and the positive sign represents tensile residual stress, while ($\sigma_c$) and the negative sign represents compressive residual stress. This model is widely used in the international literature according to the recommendations of the ECCS (European Convention for Constructional Steelworks) [9] and prEN1993-1-14 [10]. The details of this model are available in Table 3. For NSS, the tensile stress is taken equal to the yield strength of the section and the compressive stress is taken according to Table 3, $a$ and $b$ are the parameters defining the distance of each plate subjected to tensile stresses near each corner of the section. The $H/t$ ratio for the vast majority of sections under this study is larger than 40 to study class 4 slender sections.

Different studies have shown that the compressive residual stresses in the HSS are less severe than NSS due to different reasons such as better fabrication processes and better welding techniques [20,21]. Therefore, a value of 0.13*355 MPa is taken as compressive residual stress for all HSS sections and $f_y$ as tensile residual stress. The tensile zone is determined based on the equilibrium between tensile and compressive residual stresses.

**Table 2**
Material properties for different types of steel.

| Steel grade | Yield strength ($f_y$) (MPa) | Ultimate strength ($f_u$) (MPa) |
|---|---|---|
| S500 | 500 | 625 |
| S690 | 690 | 850 |
| S960 | 960 | 1115 |

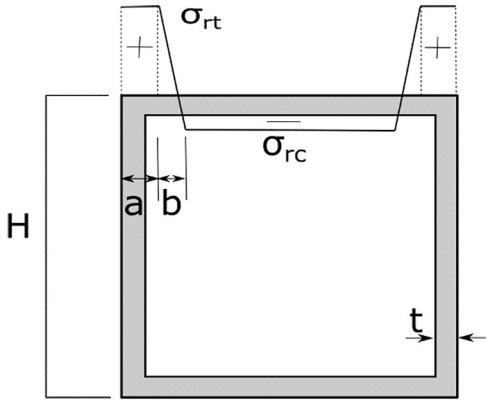


**Fig. 5.** The applied residual stress model for welded box-section columns [10].

**Table 3**
Parameter values for residual stress model according to ECCS [9].

| $H/t$ | Welding type | $\sigma_{rt}/f_y$ | $\sigma_{rc}/f_y$ | $a$ | $b$ |
|---|---|---|---|---|---|
| 10 | – | 1.0 | −0.60 | 0 | – |
| 20 | Heavy weld | 1.0 | −0.82 | 3 $t$ | 3 $t$ |
| 20 | Light weld | 1.0 | −0.29 | 1.5 $t$ | 1.5 $t$ |
| 40 | Heavy weld | 1.0 | −0.29 | 3 $t$ | 3 $t$ |
| 40 | Light weld | 1.0 | −0.13 | 1.5 $t$ | 1.5 $t$ |

### 3.4. Validation of the numerical model

The accurate behaviour of the numerical model can be verified by comparison with experimental results. This comparison includes both the behaviour of column under buckling, the ultimate force that is obtained during the tests as well as the axial deformations. To make sure that the numerical model accurately simulates the real structural behaviour and align with the experimental results, the measured material and geometrical properties are used in the numerical model. In the current study, four different research programs are used to validate the established numerical model. Approximately four samples were taken from each research program, as shown in Table 4. The first set consists of four samples that are taken from Chiew's research work [15]; this set is made of S235 steel welded box-sections with the same section width of 80 mm and varying the length of the column to produce different global slenderness ranging from $\bar{\lambda}_g$ = 0.37 to 0.59 and a constant local slenderness of $\bar{\lambda}_p$=0.71. The second set is taken from Lu Yang research program [12] consists of two rectangular cross-sections with relatively large local slenderness ratios $\bar{\lambda}_p$ = 1.5 − 1.78 . The third set contains S500 steel grades that are taken from Schillo's research program [5], box-sections with a nominal width of 160 mm was used with different column lengths to produce different global slenderness ranging from $\bar{\lambda}_g$ = 0.33 to 0.44 and an approximately constant local slenderness of $\bar{\lambda}_p$=1.06. The fourth set is taken from Khan's research program investigating S700 steel grade and different box-section widths and lengths to cover larger global and local slenderness ranges [11]. The fourth set is again taken from Schillo's research program [5], studying S960 steel grade with global slenderness ranging from $\bar{\lambda}_g$ = 0.15 to 0.42 and local slenderness of $\bar{\lambda}_p$=1.25. The full details of each test are included in Table 4, showing the steel grade, the global slenderness $\bar{\lambda}_g$, the local slenderness $\bar{\lambda}_p$, section width $b$, height $h$, thickness $t$, length $L$, yield strength $f_y$, ultimate strength $f_u$, the local imperfection scaling factor $f_{loc}$ applied in the numerical model as ($b/f_{loc}$),the ultimate load from the experiments $F_{u,exp}$, and the ultimate load from numerical calculations $F_{u,num}$. Validation of the model against the experimental tests is done using the previously presented material and residual stress models, depending on the measured material properties. All the measured values are applied according to the experimental research programs. The global imperfection that is utilised in this process is L/1000, with the actual combinations of geometrical local imperfections and residual stress, developed by the authors in a previous research program [7]. The applied actual imperfections are shown in Table 4, considering the physically possible imperfection of $\pm b/125$ according to EN 1090–2:2018 Table B.4 No. 3 [22]. Two samples are shown in Fig. 6 for the comparison between the numerical and the experimental results. The figure on the left shows a test result taken from Khan's research program [11]. The figure on the right-hand side is from Schillo's research program [23]. Both numerical results show a very reliable estimation of the behaviour and the buckling capacity of the experimental tests that is going an interaction buckling for the first case and local buckling for the second case, which proves the applicability and reliability of the numerical model. The interaction buckling mode is shown in Fig. 7, showing both the deformation as well as the Von-Mises stresses for a specimen taken from Khan's research program /S700–150–4.92-2512/ [11].

The results in Table 4 prove the numerical model is providing reliable results, as the numerical tests are done with this set of combinations of global and local imperfections as well as residual stresses. It is also

**Table 4**
Results of the model validation.

| Steel grade | $\lambda_g$ | $\lambda_p$ | $b$ (mm) | $h$ (mm) | $t$ (mm) | $L$ (mm) | $f_y$ (MPa) | $f_u$ (MPa) | Loc. Imp. Sca. Fa. ($f_{loc}$) | $F_{u,exp}$ (kN) | $F_{u,num}$ (kN) | $\frac{F_{u,num}}{F_{u,exp}}$ |
|---|---|---|---|---|---|---|---|---|---|---|---|---|
| S235 | 0.37 | 0.71 | 80 | 80 | 2 | 1100 | 261 | 360 | 2130 | 159 | 150.75 | 0.95 |
| S235 | 0.47 | 0.71 | 80 | 80 | 2 | 1500 | 261 | 360 | 2130 | 140 | 141.69 | 1.02 |
| S235 | 0.59 | 0.71 | 80 | 80 | 2 | 1850 | 261 | 360 | 2130 | 143 | 134.51 | 0.94 |
| S235 | 0.50 | 0.71 | 80 | 80 | 1.4 | 1850 | 261 | 360 | 2130 | 72 | 72.31 | 1.01 |
| S235 | 0.21 | 1.78 | 251.4 | 491 | 5.44 | 4378 | 309 | 458 | 125 | 1287 | 1268 | 0.98 |
| S355 | 0.24 | 1.51 | 209.5 | 403 | 5.82 | 3582 | 385 | 545 | 125 | 1456 | 1533 | 1.05 |
| S500 | 0.33 | 1.06 | 159.75 | 159.5 | 4.1 | 1599 | 562 | 640 | 633 | 880.3 | 948 | 1.08 |
| S500 | 0.37 | 1.07 | 160 | 159.25 | 4 | 1800 | 562 | 640 | 606 | 883.9 | 925 | 1.05 |
| S500 | 0.40 | 1.08 | 160 | 159 | 4 | 2000 | 562 | 640 | 599 | 858.2 | 899 | 1.05 |
| S500 | 0.44 | 1.08 | 159.25 | 159.25 | 4 | 2198 | 562 | 640 | 600 | 828.9 | 889 | 1.07 |
| S700 | 0.28 | 1.22 | 199 | 199 | 4.9 | 1512 | 762 | 819 | 147 | 1733 | 1735 | 1.00 |
| S700 | 0.45 | 0.90 | 149 | 149 | 4.9 | 1512 | 762 | 819 | 515 | 1800 | 1698 | 0.94 |
| S700 | 0.57 | 0.74 | 125 | 125 | 4.9 | 1512 | 762 | 819 | 400 | 1659 | 1593 | 0.96 |
| S700 | 0.45 | 1.22 | 199 | 199 | 4.9 | 2512 | 762 | 819 | 125 | 1598 | 1626 | 1.02 |
| S700 | 1.7 | 0.42 | 75 | 75 | 4.9 | 2512 | 762 | 819 | 400 | 467 | 439 | 0.94 |
| S700 | 1.75 | 0.58 | 99.4 | 99.4 | 4.9 | 3512 | 762 | 819 | 400 | 499 | 542 | 1.08 |
| S960 | 0.15 | 1.25 | 137 | 137 | 3.9 | 470 | 980 | 1024 | 125 | 1444.1 | 1298 | 0.90 |
| S960 | 0.23 | 1.17 | 136 | 136 | 4.2 | 728 | 980 | 1024 | 178 | 1400.4 | 1383 | 0.99 |
| S960 | 0.42 | 1.24 | 137 | 137 | 4 | 1299 | 980 | 1024 | 132 | 1390.5 | 1223 | 0.88 |

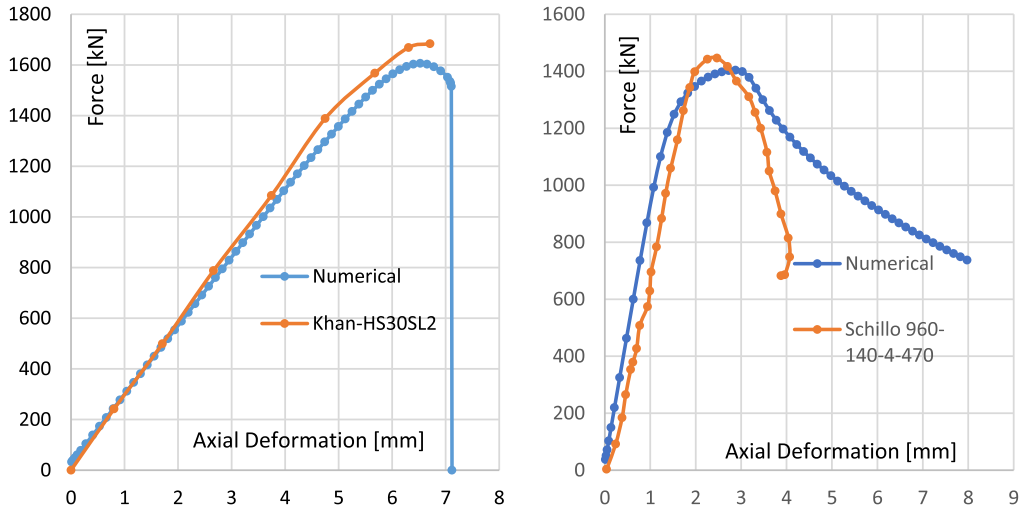


**Fig. 6.** Comparison of measured and computed load-deformation curves: a) Khan's test specimen S700–150–4.92-2512 [11] and b) Schillo's test specimen S960–140–4-470 [23].

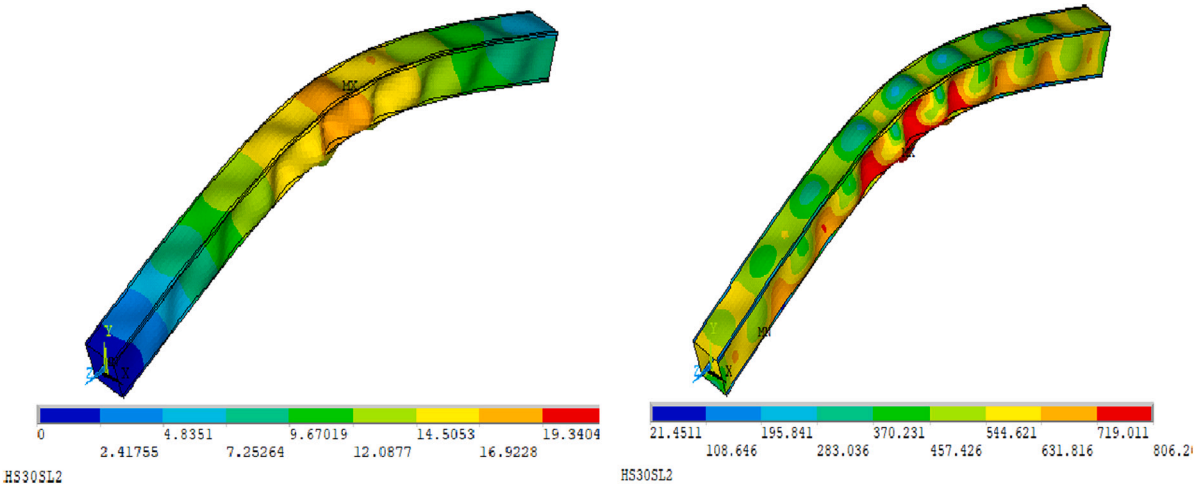


**Fig. 7.** Obtained failure mode for interaction buckling at the final loading step of Khan's test specimen S700–150–4.92-2512 [11]; a) deformed shape, b) Von-Mises stresses.

worth mentioning that some tests might have some uncontrolled eccentricities during load application that cause lower or higher capacity compared to the numerical model, where only pure compression and initial geometric imperfections were modelled.

## 4. Results of the numerical parametric study

### 4.1. Parameters used in the numerical parametric study

The numerical parametric study aims to create a large database to study the interaction buckling and propose a design formula for columns under pure compression made of normal and high strength steel welded box-section columns. The analysed cross-sections have $b/t$ ratio larger than 40 with a local slenderness ratio ($\bar{\lambda}_p$) larger than 0.7 and global slenderness ratio ($\bar{\lambda}_g$) larger than 0.2. Only square box-section columns are investigated within the current parametric study covering a wide range of width-to-thickness ratios and cross-section dimensions. The local slenderness ratio is changed between 0.6 and 2.8. The global slenderness ratio is changed between 0.1 and 2.6. The width of the analysed panels is varied between 200 mm to 450 mm. The thickness of the plates is changed between 2.5 and 12 mm with 0.5 mm increment resulting in different local slenderness ratios. The lengths of the columns are varied between 750 mm and 20,000 mm, resulting in a different global slenderness ratio for each cross-section. The parametric study and the evaluation of the results are divided into two parts, the first part is concerned with NSS (S235, S355, and S460) material, and the second part is considering HSS (S500, S700, and S960) materials, so a total of six different steel grades are covered in the current study. The applied geometries, a combination of $b = h$ and $t$ values are given in Table 5.

More than 2000 GMNI analyses are performed in the current research program, investigating 280 different sections to determine the interaction buckling resistance of columns under pure compression. Within the numerical parametric study, at first, the two boundaries: (i) pure local and (ii) pure global buckling, are investigated separately to prove the applicability of the numerical model for both failure modes and check the resistance models. Then the interaction behaviour is analysed on the same numerical model to improve the interaction buckling resistance model.

### 4.2. Local buckling behaviour

The local buckling behaviour was studied previously by the authors in a more detailed manner, results are published in a separate paper [7]. Here only the final results and the calculated buckling reduction factors

**Table 5**
Geometrical properties of the analysed cross-sections.

| | $b = h$ [mm] | thickness values [mm] | Lengths |
|---|---|---|---|
| 1 | 200 | 2.0; 2.5; 3.0; 3.5; 4.0; 4.5; 5.0; 5.5; 6.0; 6.5; | 750;1750;2500;3000;3750;5000; 6250;7500;8750;10,000;11,250; 12,500;15,000;17,500;20,000 |
| 2 | 250 | 2.0; 2.25; 2.5; 2.75; 3.0; 3.25; 3.5; 4.0; 5.0; 6.0; 7.0; 8.0 | |
| 3 | 300 | 2.75; 3.0; 3.5; 4.0; 4.25; 4.5; 4.75; 5.0; 5.25; 5.5; 5.75; 6.0; 6.5; 7.0; 8.0; 9.0 | |
| 4 | 350 | 2.75; 3.0; 3.5; 4.0; 4.5; 5.0; 5.5; 6.0; 6.5; 7.0; 8.0; 9.0; 10.0 | |
| 5 | 400 | 3.5; 3.75; 4.0; 4.25; 4.5, 4.75; 5.0; 5.5; 6.0; 6.5; 7.0; 8;0 | |
| 6 | 450 | 3.75; 4.0; 4.25; 4.5; 4.75; 5.0; 5.25; 5.5; 5.75; 6.0; 6.5; 7.0; 8.0; 9.0; 10.0; 11;0 | |

All geometries are investigated using steel grades of:
NSS: S235, S355, S460; HSS: S500; S700; S960

are presented compared to two buckling curves, which are found as the more accurate and reliable design resistance models currently. Fig. 8 shows the local slenderness ratio on the horizontal axis and the buckling reduction factor on the vertical axis. The two buckling curves are (i) the buckling curve of EN1993-1-5 Annex B, which is proposed for the square box-section columns by the Eurocode and (ii) the buckling curve developed by Schillo [5], which is found as the most reliable buckling curve currently for this column type [7,24,25]. Previous investigations of the authors [7] were executed to determine the necessary imperfection magnitude for local buckling, which local imperfection together with residual stresses and considering the manufacturing tolerances would lead to accurate local buckling resistance. The local buckling resistance considered to be accurate has been checked and statistically evaluated by Schillo in 2017 [5]. Large test database from all over the world for NSS and HSS box-sections columns are gathered by Schillo. That database has been statistically evaluated and a reliable design buckling resistance curve has been proposed. This curve can be seen by red in Fig. 8. Applying the previously developed combinations of imperfections and residual stresses by the authors [7], the obtained results prove the applied numerical model provides close resistances to this accurate buckling curve and provides reliable buckling resistances fitting to the analytical design approach.

### 4.3. Global buckling behaviour

Cross-sections not sensitive to local buckling are also investigated, and the flexural buckling resistances are determined by the numerical model. The numerical model contained L/1000 geometric imperfections and residual stresses. Results are presented in Fig. 9, proving that the flexural buckling resistance provided by the numerical model is close to the buckling curve b of the EN 1993-1-1, in which the buckling curve is tabulated for this column type.

### 4.4. Interaction between local and global buckling

After proving the numerical model fits the laboratory test results and provides reliable buckling resistances for local as well as for global buckling, the interaction buckling resistances are determined for all column geometries listed in Table 5.

At first, the obtained buckling resistances are compared to the current resistance model of the EN 1993-1-1 and EN 1993-1-5 design rules. Fig. 10 shows the comparison between the calculated buckling resistance according to Eurocode on the horizontal axis calculated using the Winter-type buckling curve available in the EN1993-1-5 [2] and the numerically computed buckling resistance on the vertical axis. It can be seen that the average value of the resistances fits quite well with the Eurocode-based calculation results. However, some results overestimate the buckling resistance, while others underestimate it with a large scatter. It is known from previous research results that; Winter-type curve is overestimating the local buckling resistance (giving average value and not lower characteristic resistance values) as shown by different previous studies. The current results prove, it also has a significant effect on the interaction resistance as well and the buckling curve modification is important for the interaction buckling case as well.

Therefore, a similar comparison is executed by modifying the local buckling resistance curve to the Annex B curve, which will be given in the second generation EN 1993-1-5. Fig. 11 shows the comparison of the numerical results to the modified Eurocode-based buckling resistance. It can be noticed that all the calculated resistances are on the safe side. However, a similar scatter remained, as obtained in Fig. 10. It shows that the real physical behaviour is not captured, and the interaction buckling is not correctly considered within the standardized resistance calculation process, which might be revised and improved. In order to achieve a better fit and see the differences, all ratios between the standardized and numerically calculated buckling resistances are calculated and presented in Fig. 12, depending on the global and local slenderness ratio on a three-dimensional surface. Fig. 13 shows the results depending only on

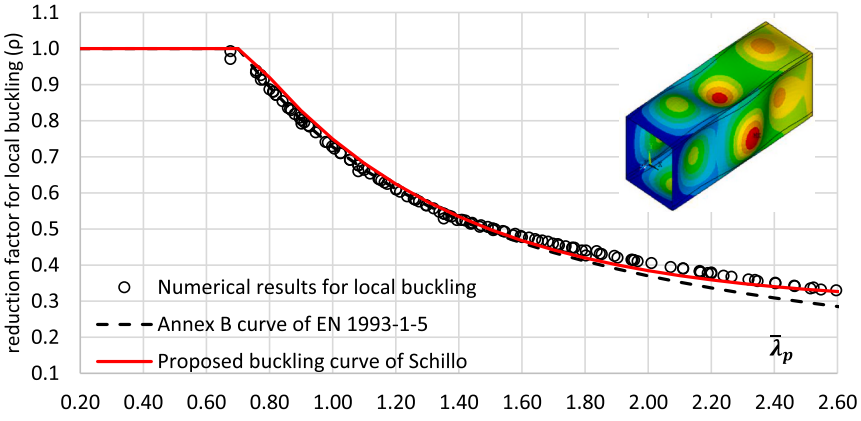


**Fig. 8.** Numerically calculated local buckling resistances compared to buckling curves.

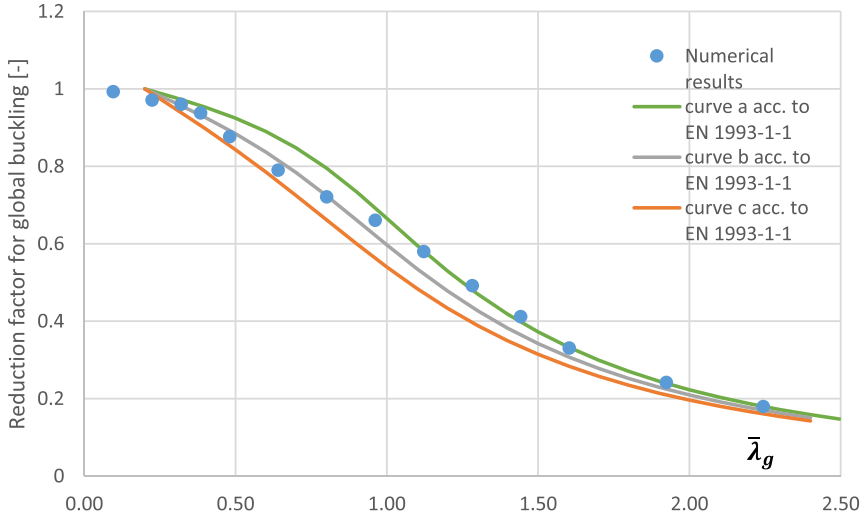


**Fig. 9.** Numerically calculated global buckling resistances compared to buckling curves.

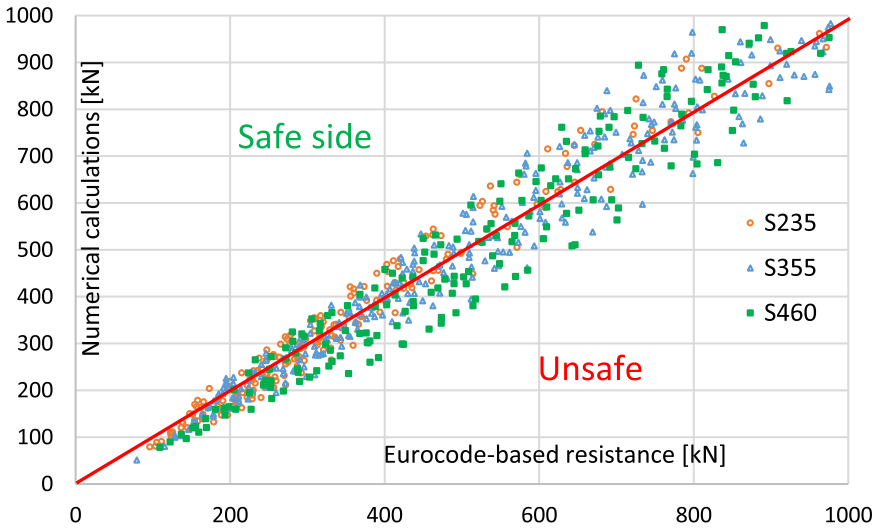


**Fig. 10.** Comparison of the numerically calculated and the Eurocode-based resistance model considering the Winter-type buckling curve in the local buckling resistance calculation.

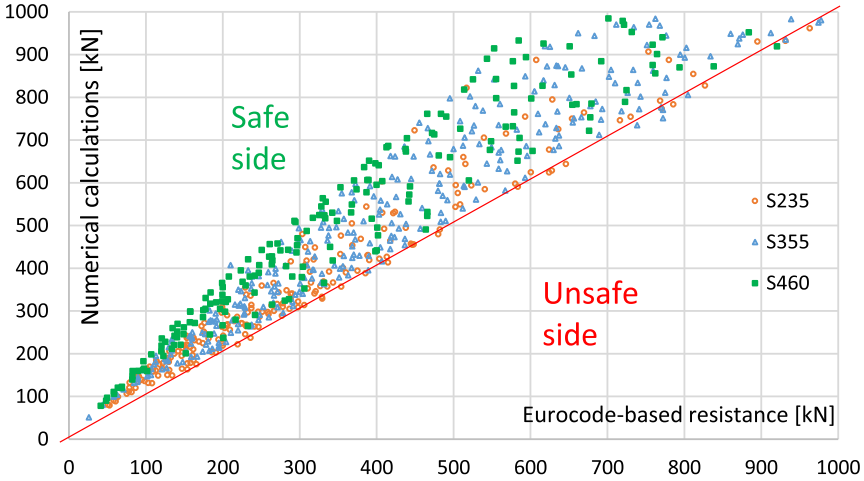


**Fig. 11.** Comparison of the numerically calculated and the Eurocode-based resistance model considering the Annex B curve in the local buckling resistance calculation.

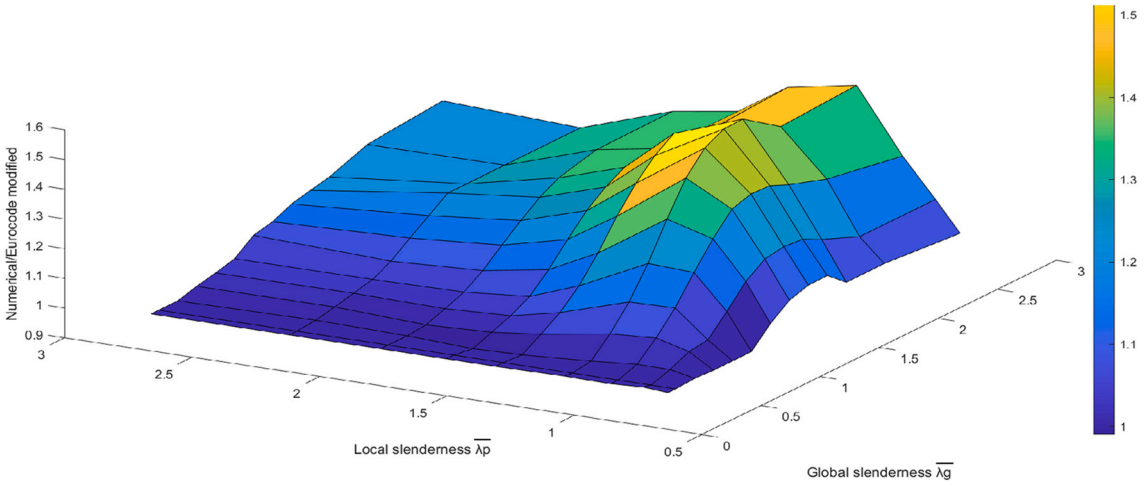


**Fig. 12.** Relationship between the ratio of numerical results to Eurocode-based interaction buckling resistance considering Annex B curve for local buckling resistance – 3D diagram.

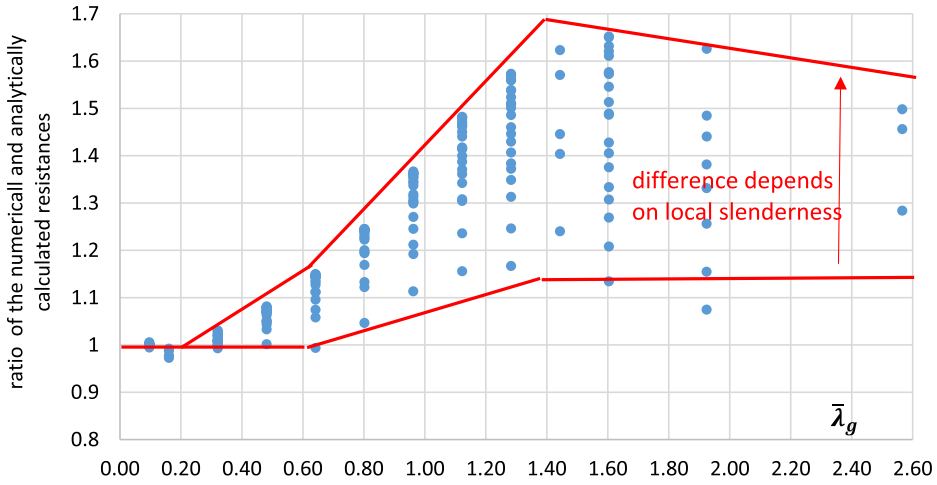


**Fig. 13.** Relationship between the ratio of numerical results to Eurocode-based interaction buckling resistance considering Annex B curve for local buckling resistance – 2D diagram.

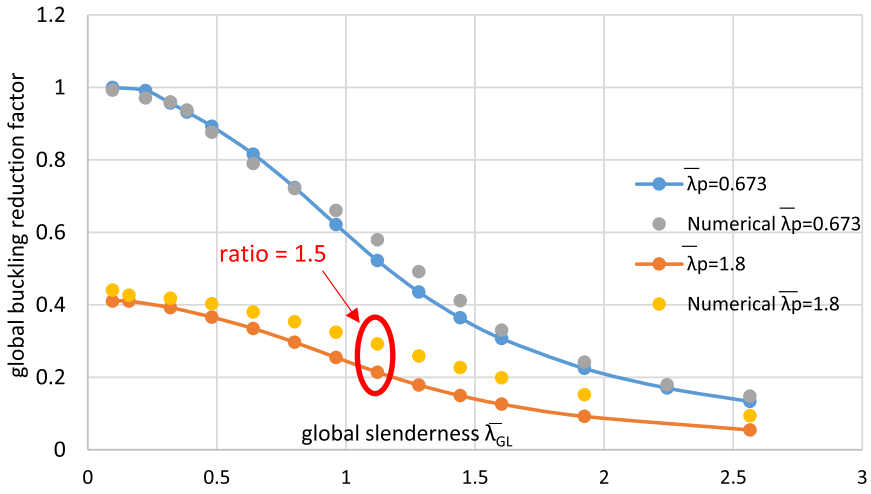


**Fig. 14.** The normalized capacity of a welded box section with respect to the global slenderness range for two slender sections with two different local slenderness.

the global slenderness ratio and indicating the maximum difference between the numerically and analytically calculated resistances. These plots highlight that the ratios for the pure local and global buckling are close to 1.0. However, in the interaction domain, the difference can reach up to 50–70% strongly depending on the local and global slenderness ratio.

The largest difference is obtained within the slenderness ratio ranges of $\lambda_{GL} = 1.0–2.0$ and $\lambda_p = 1.0–1.5$. This is the slenderness range where the residual stresses have the most significant effect on the buckling resistance, and this range is often used in the practical design. It has been previously shown by Degée et al. [6] that previous numerical calculations considered the residual stresses twice using equivalent geometric imperfections for the global and local buckling as well. The current study solves this issue and determines the correct resistances with the numerical model, making the buckling resistance model improvement possible. Results also show that the difference between the numerically and the analytically calculated resistances does not depend on the yield strength for steel grades of S235 – S460.

To show the obtained differences more understandably, a comparison is made for two cross-sections with significantly different local slenderness ratios ($\bar{\lambda}_p = 0.676$ and $\bar{\lambda}_p = 1.8$). The obtained results are compared and presented in Fig. 14 in the function of the global slenderness ratio. The vertical axis shows the normalized capacity calculated by the modified Eurocode-based resistance model, and the horizontal axis shows the global slenderness ratio. It can be seen that the difference between the applied buckling curve for the interaction behaviour and the numerical resistances significantly depend on the local as well as on the global slenderness, which should be considered more accurately in the improved resistance calculation method. The difference between the numerical calculation and the analytical solution is significantly larger for larger local slenderness values, which proves that the combination of the local and global buckling behaviour has a significant impact on each other.

## 5. Comparison with the available methods in the literature

In this section, three previously developed resistance models are compared to the numerical results. The three resistance models are proposed by Schillo [23], Degée [6] and Young [16]. The proposed method of Schillo is developed for high strength steel columns to take the effect of the interaction buckling and implement the loss of stiffness caused by local buckling in the calculation as an equivalent local imperfection factor $e_p$. The comparison of the numerical results to the analytically calculated values is presented in Fig. 15. Results show that Schillo's [23] resistance model, which uses the Annex B curve to estimate the effective area of the sections, generates reliable results for a large parameter range, follows the trend of the buckling resistance and fits the average resistance values. However, the obtained scatter within the results is still significant.

The design proposal of Degée et al. was developed for the local slenderness range $\bar{\lambda}_p = 0.7$ to 1.1 and the global slenderness of $\bar{\lambda}_g = 0.4$ to 1.4, while in this research, it was tested against a larger slenderness range, up to 2.7 in local slenderness and up to 2.6 in global slenderness. To check the validity of the Degée's resistance model against the performed numerical parametric study, a comparison was made and shown in Fig. 16.

From the obtained results, it can be concluded the proposed equation follows the trend of the numerical calculations. It presents an average solution where some results are overestimated, and others underestimated. Additionally, this method has also a significant scatter compared to the numerical results. This can be due to the fact that different proposed combinations of residual stresses and geometric imperfections were adopted in the numerical study, which was L/1000 for global imperfection and b/1000 for local imperfection with residual stresses. In contrast, in the current research, a value of L/1000 for global imperfection and the actual imperfection based on Annex B curve for local imperfections is applied with residual stresses. The differences within the applied imperfections can lead to different buckling resistances. These results also show the importance of the local imperfection in the numerical analysis that can lead to quite large differences in the interaction buckling resistance.

Fig. 17 shows the same comparison to Young's resistance model. Results prove this method shows a large scatter compared to the numerical model and comparing to the previous design models, where the majority of the results lie on the safe side but with large differences in the obtained results. A clear trend can be seen in Fig. 17 that Young's method yields a buckling capacity of approximately 50–60% of the numerically calculated values, as shown by the black line on the graph.

## 6. Improved resistance model

Observations between the numerical and analytical resistances presented in the previous sections, especially shown in Figs. 12-13 proves that the modification factor for the local or global buckling reduction factors should depend on both the local and global slenderness. Previous modifications mainly applied a modification factor depending on the local slenderness and did not consider the global buckling behaviour. Therefore, in the current study, an improved resistance model is

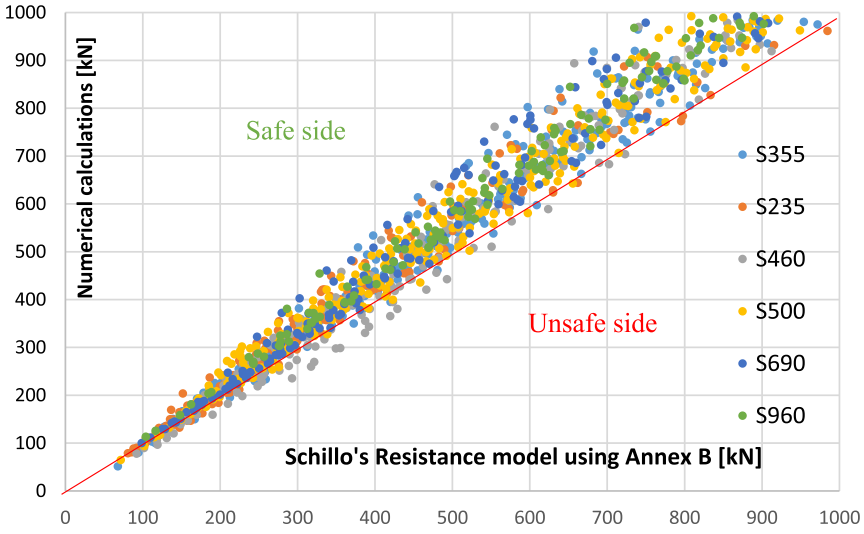


**Fig. 15.** Comparison of Schillo's resistance model and the numerical results.

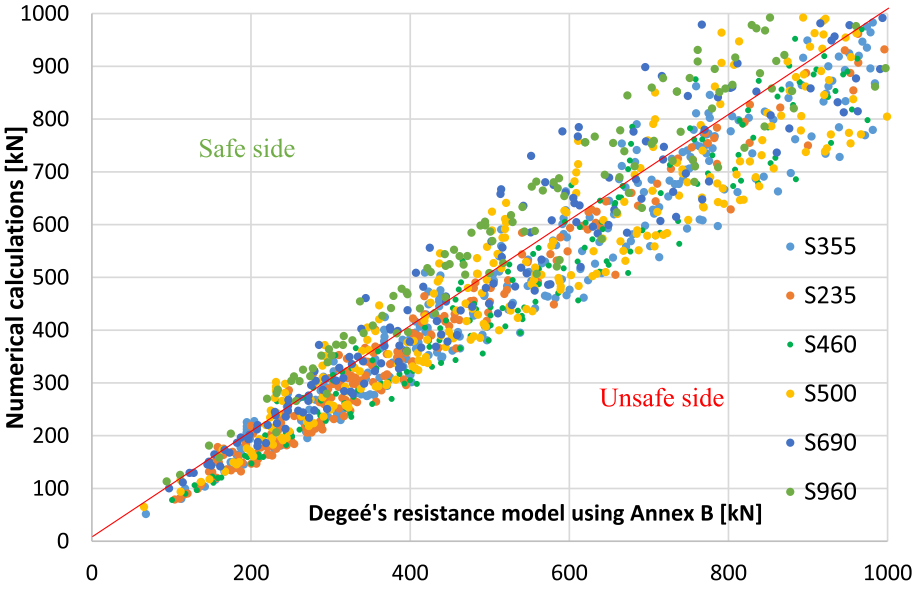


**Fig. 16.** Comparison of Degée's resistance model and the numerical results.

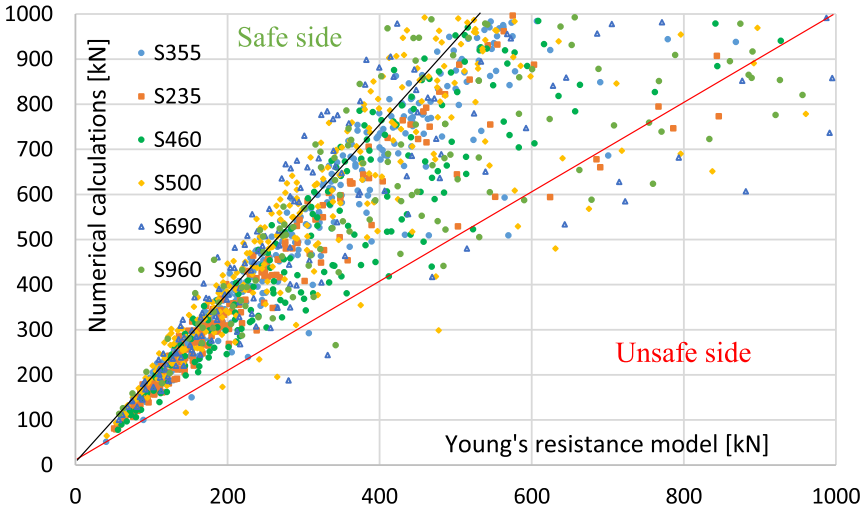


**Fig. 17.** Comparison of Young's resistance model and numerical results.

developed containing a modification factor depending on the global and local slenderness ratios as well.

The results of the numerical study were used to create the best fit resistance function. The authors wanted to keep the general calculation procedure of the Eurocode, and Eq. (10) is extended by a new modification factor, which depends on the global and local slenderness of the column under investigation. The authors also wanted to eliminate the iterative way of the resistance calculation. Therefore, the interaction buckling resistance can be determined within one step using the local and global buckling resistances and a new modification factor ($f_{mod}$). The new design process is given by Eqs. (32)–(34). The modification factor ($f_{mod}$) depends only on the local ($\bar{\lambda}_p$) and global ($\bar{\lambda}_g$) slenderness ratio. For better understanding ability, the slenderness effects are separated into two equations (Eqs. (33)–(34)). The local buckling modification factor ($f_{max}$) can be calculated by using Eq.(34), taking into account the effect of local buckling depending on the local slenderness ratio ($\bar{\lambda}_p$). The interaction modification factor ($f_{mod}$) can be calculated by using Eq. (33), taking into account the interaction effect through the consideration of the global slenderness ($\bar{\lambda}_g$) and $f_{max}$.

Within the improved resistance model, the global buckling reduction factor $\chi$is calculated using the column buckling curve "b" according to EN1993-1-1 [1]. The effective area $A_{eff}$ is determined using the Annex B buckling curve of EN1993-1-5 [2]. It is worth mentioning that the current proposal is valid for both normal and high strength steel, as it will be shown later in the following section.

$$N_{b,int,Rd} = f_{mod} \cdot \chi \cdot \frac{A_{eff} \cdot f_y}{\gamma_{M1}} = f_{mod} \cdot \chi \cdot \frac{\rho A f_y}{\gamma_{M1}} \tag{32}$$

Where:

$$f_{mod} = \begin{cases} 1, \bar{\lambda}_g \le 0.4 \\ 1 + (\bar{\lambda}_g - 0.4) \cdot (f_{max} - 1), 0.4 < \bar{\lambda}_g < 1.4 \\ f_{max}, \ \bar{\lambda}_g \ge 1.4 \end{cases} \tag{33}$$

$$f_{max} = \begin{cases} 1, \bar{\lambda}_p \le 0.67 \\ 1 + (\bar{\lambda}_p - 0.67) \cdot 1.36, 0.67 < \bar{\lambda}_p < 1 \\ 1.45, \ \bar{\lambda}_p \ge 1 \end{cases} \tag{34}$$

$\chi$ reduction factor related to global flexural buckling according to EN 1993-1-1,

$\rho$ reduction factor related to local plate buckling according to EN

1993-1-5

– in the present study Annex B buckling curve is used in the $A_{eff}$ calculation,

$\bar{\lambda}_p$ local slenderness ratio according to Eq. (8),

$\bar{\lambda}_g$ global slenderness ratio according to Eq. (5) without considering $A_{eff}$. in the global buckling behaviour.

It should be mentioned the new design model has a clear physical background and fits the boundaries of global and local buckling cases, for which the current design approaches are proved safe-sided and reliable. Therefore, in the improved design model if $\bar{\lambda}_p \leq 0.67$ or $\bar{\lambda}_g \leq 0.2$ the modification factor is 1.0, leading to the pure flexural buckling case or the pure local buckling cases, respectively. The maximum improvement within the interaction buckling resistance is achieved in the parameter range where $\bar{\lambda}_p \geq 1.0$ and $\bar{\lambda}_g \geq 1.4$, meaning that for columns having large local and global slenderness ratios, the interaction has the largest effect, and the largest modification factor is required to consider it. Within the intermediate slenderness regions, the influence of the interaction is more or less linear and clearly depends on both the local and global slenderness ratios, as considered by Eqs. (33)–(34). Visualization of the modification factor depending on the local and global slenderness ratios is given in Fig. 18. Within the calculation process, the local and global buckling reduction factors and their calculation methods are completely separated; no interaction is considered in the $\chi$ and $\rho$ calculation. The interaction effect is entirely considered in the modification factor ($f_{mod}$). This separation technique improves the ease-of-use of the design process and ensures highly accurate results, as proved in the following.

### 6.1. Validation of design proposal for NSS grades

The proposed design method is compared to the numerically calculated buckling resistances; the comparison is shown in Fig. 19 for normal strength steel grades, where the horizontal axis represents the calculated resistance according to Eqs. (32)–(34), while the vertical axis represents the numerical results. It can be seen that almost all the points lie above the diagonal line meaning the safe-sided region. It can be seen that the proposed method is always giving a reliable minimum estimation of the resistance with limited scattering compared to Eurocode resistance calculated using the Annex b curve. This shows that the proposed fit is significantly reliable, as it yields safe resistances compared to the obtained resistance of the numerical analysis,

### 6.2. Validation of design proposal for HSS grades

Results show that the proposed resistance model is also valid for columns made of HSS grades as well. Comparison of the numerical and analytical resistances are summarized in Fig. 20. It is worth mentioning that an upgrade from buckling curve “b” to curve “a” in Eq. (32) would be feasible for S960 to achieve a more accurate fit as different studies proposed previously.

The statistical evaluation of the obtained results is also executed, and the relevant values are given in Table 6. The mean values, standard deviation and coefficient of variation (CoV), the minimum and the maximum values of the results are shown in Table 6. The given values are calculated for the ratio of the resistances determined by the developed enhanced analytical model, or by the Eurocode-based original design equations using the Winter-type or Annex B buckling curve, divided by the numerical results. Results show the improvement achieved by the proposed method to decrease the scattering of the results compared to the cases of applying the Eurocode-based approach using the Winter-type curve or Annex B curve. As it can be seen, the developed model shows a better mean value and a smaller CoV compared to the current Eurocode based solutions, irrespective of the buckling curves. The developed model is showing the best results with the least scattering for NSS. Although the statistical measures for the HSS show larger scattering compared to NSS, the proposed model is still valid and showing a good agreement with the numerical tests and nearly all the results are on the safe side.

## 7. Conclusions

Previous research papers criticised the design method of EN1993-1-1 [1] and EN 1993-1-5 [2] regarding the local and global interaction buckling resistances for welded box-section columns subjected to pure compression. Therefore, the current research work investigated the interaction buckling capacity of welded square box-section columns under pure compression utilising a GMNIA technique and FEM based design approach to accurately determine the interaction buckling resistance of slender columns. The executed research work included developing a numerical model that can capture the combined behaviour of both global and local buckling and can estimate the interaction buckling resistance. The numerical model has been extensively validated and verified by the authors for the local, global and interaction buckling capacities separately. A new approach is applied in the numerical model to consider accurate geometric imperfections and residual stresses to eliminate the duplicated effect of residual stresses, which

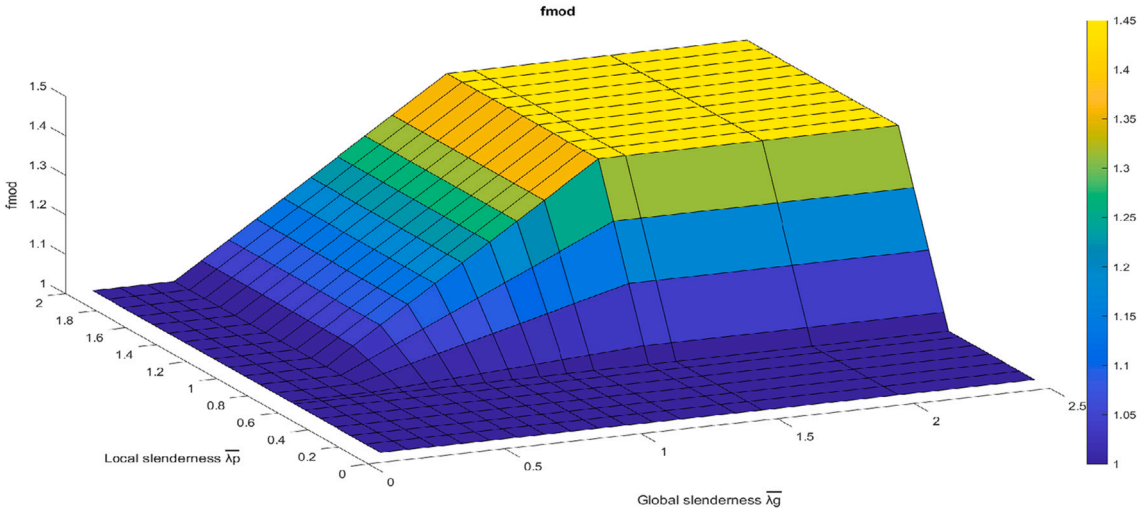


**Fig. 18.** Proposed modification factor depending on the local and global slenderness ratios.

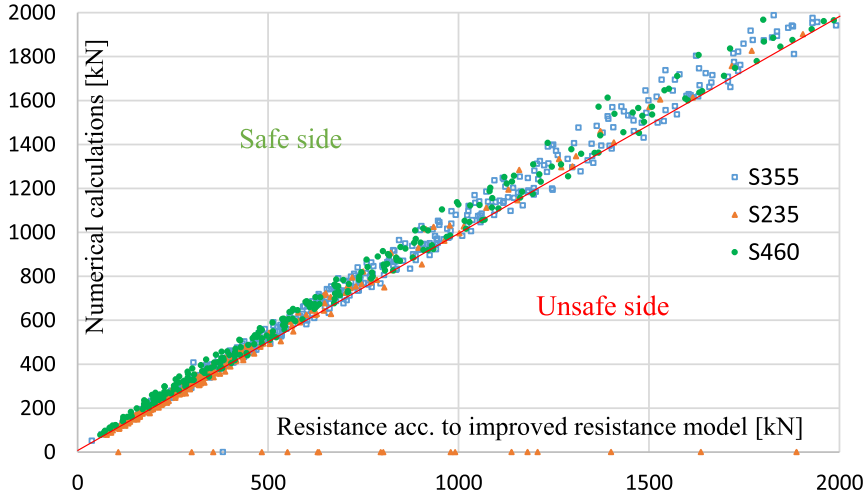


**Fig. 19.** Comparison of the numerical and analytical buckling resistances for NSS.

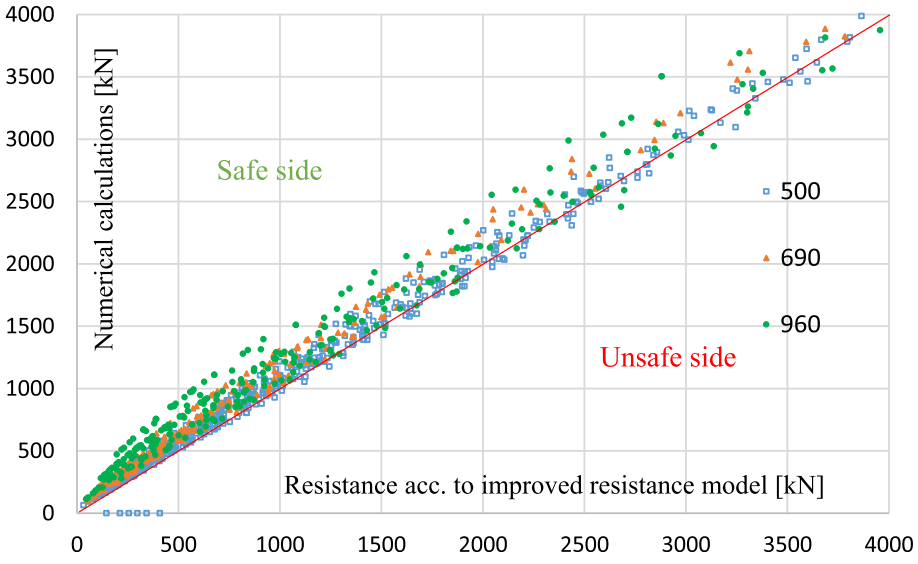


**Fig. 20.** Comparison of the numerical and analytical buckling resistances for HSS.

**Table 6**
Statistical measures of the numerical results.

| | NSS | | | HSS | | |
|---|---|---|---|---|---|---|
| | Dev. Model/Num. Model | Winter/Num. Model | Annex b/Num. Model | Dev. Model/Num. Model | Winter/Num. Model | Annex b/Num. Model |
| Mean | 0.946 | 0.936 | 0.799 | 0.899 | 0.899 | 0.750 |
| Standard Deviation | 0.056 | 0.150 | 0.132 | 0.090 | 0.150 | 0.137 |
| CoV | 0.060 | 0.160 | 0.165 | 0.100 | 0.167 | 0.183 |
| Min | 0.848 | 0.645 | 0.516 | 0.781 | 0.537 | 0.422 |
| Max | 1.109 | 1.204 | 1.033 | 1.091 | 1.196 | 1.036 |

importance has been highlighted in previous research works. Another improvement in the current research work is that the buckling curve for local buckling has been previously changed for welded square box-section columns, and it also has an effect on the interaction buckling resistance, which was not tested and analysed before. The current investigation considered the new buckling curve in the interaction buckling resistance calculation and approved its applicability and high accuracy as well.

A numerical parametric study was carried out using the verified and validated numerical model investigating a large range of global and local slenderness values to create a resistance database, which can be used to evaluate and improve the previously developed buckling resistance models. Using the numerical calculation results, the differences between the previous resistance models and the numerical resistances are evaluated and the correct trends depending on the local and global slenderness are determined. Based on the numerical calculations, an improved resistance model is developed given by Eqs. (32)–(34) providing highly accurate resistances for the interaction buckling problem. New improvements in the proposed equations are the following:

- Calculation of the global and local buckling reduction factors are separated, and the design calculations follow the rules of the Eurocode,
- The interaction of local and global buckling is considered by a universal modification factor ($f_{mod}$) considering both the local and global slenderness ratio,
- No iteration is necessary within the design process due to the cross-sectional changes.

## CRediT authorship contribution statement

**M. Radwan:** Methodology, Software, Validation, Formal analysis, Investigation, Resources, Data curation, Writing – original draft, Writing – review & editing, Visualization. **B. Kövesdi:** Conceptualization, Methodology, Software, Validation, Formal analysis, Investigation, Resources, Data curation, Writing – review & editing, Visualization, Supervision, Project administration, Funding acquisition.

## Declaration of Competing Interest

The authors declare that they have no known competing financial interests or personal relationships that could have appeared to influence the work reported in this paper.

*Acknowledgement*

The presented research program has been financially supported by the Grant MTA-BME Lendület LP2021-06 / 2021 "Theory of new generation steel bridges" program of the Hungarian Academy of Sciences and Stipendium Hungaricum Scholarship. Both grants are gratefully acknowledged.

## References

[1] C.E. de Normalisation, EN 1993-1-1 (2005) (English): Eurocode 3: Design of Steel Structures - Part 1–1: General Rules and Rules for Buildings, British Standards Institute, London, 2005. https://www.phd.eng.br/wp-content/uploads/2015/12/en.1993.1.1.2005.pdf.
[2] C.E. de Normalisation, EN 1993-1-5: 2006 Eurocode 3-Design of Steel Structures, Part 1.5: Plated Structural Elements, British Standards Institute, London, 2006. https://www.phd.eng.br/wp-content/uploads/2015/12/en.1993.1.5.2006.pdf (accessed May 20, 2021).
[3] X. Cao, R. Zhong, Y. Xu, C. Cheng, S. Liu, Z. Chen, S.-E. Kim, Z. Kong, Local–overall interactive buckling behaviour of 800 MPa high-strength steel welded H-section members under axial compression, Thin-Walled Struct. 164 (2021), 107793, https://doi.org/10.1016/j.tws.2021.107793.
[4] H.X. Yuan, Y.Q. Wang, L. Gardner, Y.J. Shi, Local–overall interactive buckling of welded stainless steel box section compression members, Eng. Struct. 67 (2014) 62–76, https://doi.org/10.1016/j.engstruct.2014.02.012.
[5] N. Schillo, M. Feldmann, A. Taras, Local and global buckling of box columns made of high strength steel, Universitätsbibliothek der RWTH Aachen 81 (2017) 1–304, https://doi.org/10.18154/RWTH-2017-07053.
[6] H. Degée, A. Detzel, U. Kuhlmann, Interaction of global and local buckling in welded RHS compression members, Int. Colloq. Stab. Ductility Steel Struct. 2006 (64) (2008) 755–765, https://doi.org/10.1016/j.jcsr.2008.01.032.
[7] M. Radwan, B. Kövesdi, Local plate buckling type imperfections for NSS and HSS welded box-section columns, Structures. 34 (2021) 2628–2643, https://doi.org/10.1016/j.istruc.2021.09.011.
[8] C.E. de Normalisation, prEN 1993-1-5:2024, Eurocode 3: Design of steel structures, Part 1.5: Plated structural elements, European Committee for Standardization, Brussels, 2022 (under development).
[9] ECCS, European recommendations for steel construction; buckling of steel shells, European Convention for Constructional Steelwork Brussels, 1988.
[10] C.E. de Normalisation, prEN 1993-1-14:2020: Eurocode 3: Design of steel structures, Part 1–14: Design assisted by Finite element analysis (under development), 2021.
[11] M. Khan, B. Uy, Z. Tao, F. Mashiri, Concentrically loaded slender square hollow and composite columns incorporating high strength properties, Eng. Struct. 131 (2017) 69–89, https://doi.org/10.1016/j.engstruct.2016.10.015.
[12] L. Yang, G. Shi, M. Zhao, W. Zhou, Research on interactive buckling behavior of welded steel box-section columns, Thin-Walled Struct. 115 (2017) 34–47, https://doi.org/10.1016/j.tws.2017.01.030.
[13] T. Usami, Y. Fukumoto, Local and overall buckling of welded box columns, J. Struct. Div. 108 (1982) 525–542, https://doi.org/10.1061/JSDEAG.0005901.
[14] T. Usami, Y. Fukumoto, Welded box compression members, J. Struct. Eng. 110 (1984) 2457–2470, https://doi.org/10.1061/(ASCE)0733-9445(1984)110:10(2457).
[15] S.-P. Chiew, S.-L. Lee, N.E. Shanmugam, Experimental study of thin-walled steel box columns, J. Struct. Eng. 113 (1987) 2208–2220, https://doi.org/10.1061/(ASCE)0733-9445(1987)113:10(2208).
[16] Y.B. Kwon, E.G. Seo, Prediction of the compressive strength of welded RHS columns undergoing buckling interaction, Thin-Walled Struct. 68 (2013) 141–155, https://doi.org/10.1016/j.tws.2013.03.009.
[17] ANSYS® v18, Canonsburg, Pennsylvania, USA. https://www.ansys.com/, 2021.
[18] L. Gardner, X. Yun, A. Fieber, L. Macorini, Steel design by advanced analysis: material modeling and strain limits, Engineering. 5 (2019) 243–249, https://doi.org/10.1016/j.eng.2018.11.026.
[19] B. Somodi, Flexural Buckling Resistance of High Strength Steel Welded and Cold-Formed Square Closed Section Columns, 2017.
[20] Y.-B. Wang, G.-Q. Li, S.-W. Chen, The assessment of residual stresses in welded high strength steel box sections, J. Constr. Steel Res. 76 (2012) 93–99, https://doi.org/10.1016/j.jcsr.2012.03.025.
[21] M. Khan, A. Paradowska, B. Uy, F. Mashiri, Z. Tao, Residual stresses in high strength steel welded box sections, J. Constr. Steel Res. 116 (2016) 55–64, https://doi.org/10.1016/j.jcsr.2015.08.033.
[22] EN 1090–2: 2018, Execution of Steel Structures and Aluminium Structures - Part 2: Technical Requirements for Steel Structures, Eur. Comm. Stand. CEN, 2016.
[23] N. Schillo, M. Feldmann, Interaction of local and global buckling of box sections made of high strength steel, Thin-Walled Struct. 128 (2018) 126–140, https://doi.org/10.1016/j.tws.2017.07.009.
[24] N. Schillo, A. Taras, M. Feldmann, Assessing the reliability of local buckling of plates for mild and high strength steels, J. Constr. Steel Res. 142 (2018) 86–98, https://doi.org/10.1016/j.jcsr.2017.12.001.
[25] N. Schillo, M. Feldmann, Local buckling behaviour of welded box sections made of high-strength steel: comparing experiments with EC3 and general method, Steel Constr. 8 (2015) 179–186.